X-ray back-lighter characterization for iron opacity measurements using laser-produced aluminium K-alpha emission

a K Rossall, L M R Gartside, S Chaurasia, S Tripathi, D S Munda, N K Gupta, L J Dhareshwar, J Gaffney, S J Rose, G J Tallents, et al.

X-ray back lighter characterisation for iron opacity measurements using laser produced aluminium K-alpha emission

A K Rossall[1*], L M R Gartside[1], S Chaurasia[2], S Tripathi[2], D S Munda[2], N K Gupta[2], L J Dhareshwar[2], J Gaffney[3], S J Rose[3] and G J Tallents[1]

1. *Dept. Of Physics, University of York, Heslington, York, YO10 5DD, UK*
2. *Laser and Neutron Physics Section, Bhabha Atomic Research Centre, Mumbai, 400085, India*
3. *Imperial College of Science, Technology and Medicine, Blackett Laboratory, London, SW7 2BZ, UK*

[*]Tel.: +44 1904 434619
Email address: akr500@york.ac.uk

Abstract

Aluminium K_α emission (1.5 keV) produced by an 8 J, 500 ps, Nd:Glass laser incident at 45° onto a layered target of 0.8 μm thick aluminium (front side) and 1μm thick iron (back side) has been used to probe the opacity of iron plasma. Source broadened spectroscopy and continuum emission analysis shows that whole beam self focussing within the aluminium plasma results in a two temperature spatial distribution. Thermal conduction from the laser-irradiated aluminium into the iron layer, enhanced by the whole beam self focusing, results in iron at a temperature of ~ 10 – 150 eV. The iron opacity at photon energy of 1.5 keV is shown to be strongly modified from cold values in agreement with IMP code opacities. Results presented here represent a feasibility study to seed future work using table top laser systems for plasma opacity experiments.

PACS numbers: 52.50.Jm, 52.25.Os, 52.38.Hb

1. Introduction

Experimental determinations of opacity for a range of plasma parameters are necessary for a wide range of applications. In astrophysics, knowledge of plasma opacity is required for radiation diffusion modelling of stars [1]. Opacity is of importance in inertial confinement fusion, as it is required to accurately model radiative hydrodynamics [2] and hohlraum physics [3]. Methods used previously [4, 5] to determine plasma opacity include the use of x-rays emitted from laser produced plasmas as

back-lighters to probe heated targets. More recently, EUV lasers have been utilised to probe buried layer targets heated by a laser pulse [6]. Multiple beam, high powered lasers have usually been needed to undertake opacity measurements, due to the requirement to heat the opacity target and the x-ray back-lighter source separately [4-6]. Some single laser beam plasma opacity measurements have been undertaken using recorded emission from buried layer targets. Here the plasma is assumed to be in LTE and Kirchhoff's Law is used to infer opacity from the emissivity [7]. Future techniques could involve the use of free electron lasers to investigate opacity. Recent results by Nagler et al. [8] demonstrate how aluminium turns transparent when irradiated with soft x-rays.

In this work, we report plasma opacity measurements recorded using a single laser beam to both heat material and produce the back-lighter source. We use a single target comprising two layers as a heating source for the probed material, through thermal conduction, and for the probing x-ray emission source. The iron plasma conditions are estimated using 2D fluid code simulations. With this technique, it is possible to record the opacity of colder material, where emission is too weak for single beam opacity measurements utilising Kirchhoff's Law [7].

2. Experimental Set-up

The experiment was carried out using an Nd:Glass laser system situated at the Bhabha Atomic Research Centre (BARC). This laser provides an output energy of 8 J per pulse with a duration of 500 ps. The p-polarized laser was incident onto targets at an angle of 45^{o} to the target normal and focused to a spot size of 120 µm using an f/5 lens, yielding an on target peak intensity of 1.4×10^{14} Wcm^{-2}. The targets comprised 0.8 µm thick Al, coated using a thermal evaporation plant, onto a 1 µm layer of Fe foil, supported by photo etched copper mounts with a circular target area of diameter 1 mm. The aluminium side of the targets was irradiated by the laser. Pure aluminium foils of thickness 0.8 µm, mounted in a similar manner, were used as targets for comparative purposes.

A crystal spectrometer was utilised to measure aluminium He- and Li- like lines and the solid K_{α} emission transmitted through the aluminium and iron layers. The spectrometer was positioned at the rear side of the target along the axis of the laser at 45^{o} to the target normal. Time integrated spectra in

the wavelength range 7 – 9 Å, were recorded by dispersing the x-rays with a flat TAP crystal ($2d$ = 25.75 Å) onto a P-11 phosphor screen followed by an image intensifier tube and a CCD camera (PixelFly QE). Scattered visible light was prevented from entering the spectrometer using B10 filters (aluminised polycarbonate, Alexander Vacuum Research, Inc.). The spectral resolution of the spectrometer was dominated by the source size with $\lambda/\Delta\lambda \approx 400$. Four silicon photodiodes (XUV-100, OSI Optoelectronics), under reverse bias, were used to measure the time and space integrated emissivity of the aluminium plasma. Filters of 5 μm & 20 μm Al, 5 μm Ni, and 12 μm Ti were used to control the spectral range recorded (see figure 2). The diode active area is 100mm^2, but different sized apertures were utilised to avoid detector saturation. The diodes viewed the front side of the irradiated targets.

Aluminium K_α emission, at 1.5 keV, from pure 0.8 μm thick aluminium targets was used to calibrate the backward directed emission without an iron layer so that the transmission of iron heated by thermal conduction from the aluminium plasma could be recorded when shots with the iron and aluminium targets were employed. Al K_α emission occurs during the laser pulse as it relies on the hot electron interaction with solid Al and so is used for our time integrated transmission measurements because the time of emission is well defined. Test measurement of transmission through unheated iron placed 7mm behind a pure aluminium target showed that the iron transmission, T, measured by this technique, is within 14% of the value (T=0.067) predicted by Henke et al. [9] (see figure 6).

3. Analysis

The relatively long laser pulse length of 500ps allows time for sufficient plasma expansion during the initial rise time of the pulse to provide the large under dense plasma necessary for whole beam self focussing [10]. Estimation of the ion sound speed (~8×10^4 ms^{-1}) yields a scale length of ~40μm at the peak of the laser pulse. A two temperature electron distribution is observed within the Al plasma. Source broadened spectroscopy provides an ‘emission map’ of the plasma and shows a central hot

plasma surrounded by cooler material, while measurements of continuum emission show the presence of two temperature components.

3.1 Diode Array

Continuum emission from the Al plasma is measured using filtered EUV enhanced silicon inversion layer photodiodes. Assuming Maxwellian electron distributions, the continuum emission from the Al plasma can be modelled using [11]:

$$j(\nu) = n_e n_i Z^2 \left(\frac{e^2}{4\pi\varepsilon_0}\right)^3 \frac{8\pi}{3\sqrt{3}m^2c^3}\left(\frac{2m}{\pi kT}\right)^{1/2} \exp\left(-\frac{h\nu}{kT}\right)\left[\bar{g}_{ff} + G_n \frac{\xi}{n^3}\frac{\chi_i}{kT}\exp\left(\frac{\chi_i}{kT}\right) + \sum_{p=n+1}^{\infty} G_p \frac{Z^2 R_y}{p^2 kT}\frac{2}{p}\exp\left(\frac{Z^2 R_y}{p^2 kT}\right)\right] \quad (1)$$

where m is the electron mass, R_y is the Rydberg energy, ξ is the number of holes in the ground state of principal quantum number n, $\bar{g}_{ff}$ is the free-free Gaunt factor and is assumed to be 1, G_n and G_m are bound-free Gaunt factors where $G_m = 0$ for $h\nu < Z^2R_y/m^2$ and G_m=1 (or 1.4 if $T > 400$eV) for $h\nu > Z^2R_y/m^2$, G_n=0 for photon energies less than the ground state ionisation potential χ_i, otherwise G_n=1. Analysis of the continuum emission from the Al plasma using equation 1 and comparing the ratios between diode signals indicates the requirement for two temperature regions in order to reproduce the observed signals. The ionisation level, Z, and number densities of electrons and ions, n_e and n_i, are determined by assuming LTE within that region. Adapting this model to allow for two temperature regions of T_c and T_h with relative number fraction f, and incorporating the energy dependant transmission [9] of the filters (T_f) allows for the ratio between diode channels to be determined using:

$$R = \frac{\int_0^\infty T_{f1}(\nu)[G(T_c,\nu) + f^2 G(T_h,\nu)]d\nu}{\int_0^\infty T_{f2}(\nu)[G(T_c,\nu) + f^2 G(T_h,\nu)]\,d\nu} \quad (2)$$

where

$$G(T,\nu) = Z(kT)^{-0.5}\exp\left(-\frac{h\nu}{kT}\right)\left[\bar{g}_{ff} + G_n\frac{\xi}{n^3}\frac{\chi_i}{kT}\exp\left(\frac{\chi_i}{kT}\right) + \sum_{p=n+1}^{\infty} G_p\frac{Z^2R_y}{p^2kT}\frac{2}{p}\exp\left(\frac{Z^2R_y}{p^2kT}\right)\right] \quad (3)$$

and the subscripts *f1, f2* refer to different filters.

Equation 2 is numerically integrated also taking into account the effect of the photodiode depletion depth. By comparing calculated ratios, R, to experimentally measured diode signal ratios, it is possible to deduce the parameters T_c, T_h, and f. For example, analysing the ratio between the two highest energy diode channels, R_{High}, (5µm Ni and 12µm Ti) enables a hot electron temperature, T_h, of 1keV to be deduced to within 0.1keV accuracy, as there is negligible effect on this ratio due to a change in T_c or f, as shown in figure 1.

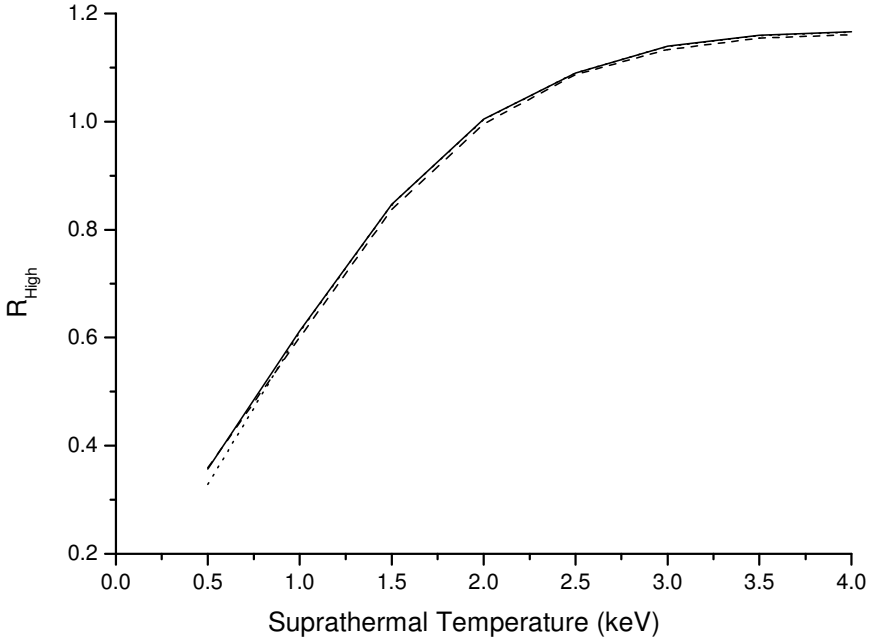

Figure 1. Variation of diode signal ratio for the two highest energy channels (5µm Ni and 12µm Ti) as a function of the hot electron temperature. The solid line represents a cold electron temperature of T_c=140eV and relative fraction of hot to cold number, f=0.008, while the dashed line represents T_c=240eV and f=0.008 and the dotted line represents T_c=140eV and f=0.05

To determine the remaining 2 parameters (T_c and f), a minimisation routine is performed using ratios from all channels to find a best fit of the model (equation 2) to the experimental data. This yields a thermal temperature of T_c=140 ± 10eV and a fraction of f = 0.008 ± 0.001, consistent over multiple shots. The peak of the spectral range detected by the diodes for the filters and experimental parameters is illustrated in figure 2. A comparison of equation (1), with temperature T_c=140eV, T_h=1keV and f=0.008, is also made on figure 2 with the total emissivity as predicted by the FLYCHK code [13]. The model shows good agreement with continuum emission, omitting line radiation as expected. When the energy dependant filter transmission is included, the integrated diode signals as predicted by our model using equation (1) and FLYCHK agree to within 4%, so our omission of the small contribution to the diode signal from line emission is not significant.

Figure 2 shows the photon energies where the filtering for each diode gives maximum recorded x-ray flux and illustrates how we can use the four diode signals to measure T_h, T_c and f. The spacing of these peaks allows the determination of the hot temperature, T_h, component (from signal ratio R for the two highest energy channels), the cold temperature, T_c, component (from the signal ratio R of the two lowest energy channels) and the ratio, f, the number of hot to cold electrons (from the ratio of the two intermediate channels).

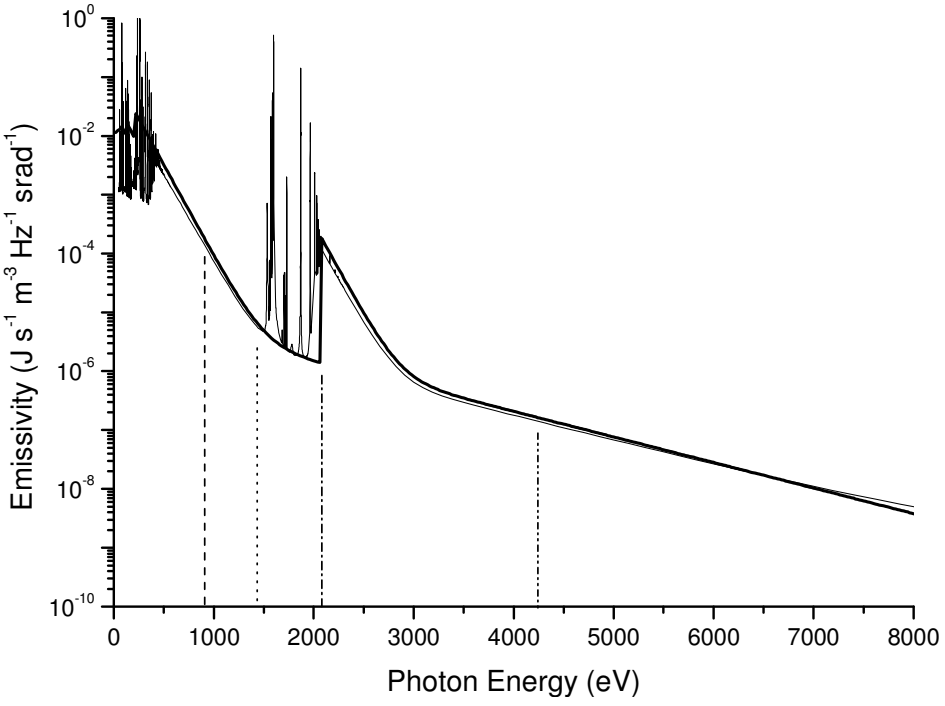

Figure 2. Continuum emission from the laser produced aluminium plasma as predicted by equation 1, incorporating two temperature regions within the plasma (thick solid line) with a comparison of total emission as predicted by FLYCHK [13](thin solid line). Conditions used are T_c = 140eV, T_h = 1000eV and f = 0.008. The peak of the transmitted emissivity curves for the diode filters of 5µm Al (dashed line), 20µm Al (dotted line), 12µm Ti (dash-dot line) and 5µm Ni (dash-dot-dot line) are indicated.

3.2 TAP Crystal Spectrometer

The recorded time integrated aluminium spectrum (see figure 3 for example) predominantly comprises a series of lines originating from helium-like and lithium-like ions. The most prominent of these lines is the He-like resonance line (w), purposefully instrument saturated to enable an improved resolution of the intercombination line (x, y) and the Li-like satellites (abcd, jkl, op, qr), (the standard letter designation used here for He-like satellite lines has been tabulated by Gabriel [12]). Line ratios between the Li-like and He-like lines enable the determination of plasma characteristics through comparison with the spectral modelling code FLYCHK [13]. Utilising the relative intensity of the He-like intercombination line and the Li-like satellites provides a useful diagnostic tool giving a measure of the electron densities and temperatures in the aluminium at the time and position of peak emission. FLYCHK does not simulate the aluminium K_α emission which is produced by the hot electron interaction with solid aluminium.

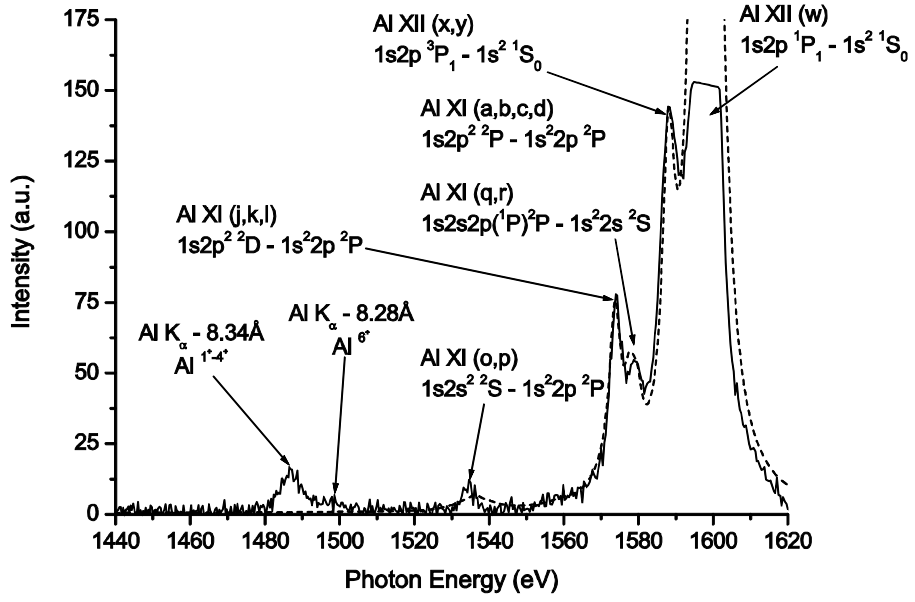

Figure 3. Experimental aluminium spectrum (solid line) and superimposed simulation (dashed line) of temperatures T_c=140 eV and T_h= 1keV using FLYCHK. The fraction of suprathermal to thermal electrons is F=0.008. [13, 14].

In order to obtain a fit to the spectra, such as figure 3, using FLYCHK, a parameter scan was performed trialling a range of temperatures (50 - 500eV) and densities (10^{12} - 10^{21} cm^{-3}). The simulated spectra were instrument broadened with our estimated resolution (~3eV) using a post-processor [15] and the peak to peak ratios were deduced and compared with the experimental spectra. A single thermal temperature component could not reproduce the observed spectra. An electron density of n_c=5x10^{20} cm^{-3} was found to best fit the spectra, consistent with the turning point density for a 45° obliquely incident 1.06μm Nd:Glass laser. As the emission is proportional to n_e^2 and n_e=5x$10^{20}$$cm^{-3}$ is the highest density directly heated by the laser, we assume emission from this single density is a reasonable approximation to a spatial integration of emission. A parameter scan of the hot electron temperature, T_h, (0.5 - 2keV) and hot to cold component fraction, f, (0.005 - 0.1) was performed and found to require T_h=1keV and f=0.008 for T_c=140eV (see e.g. figure 4).

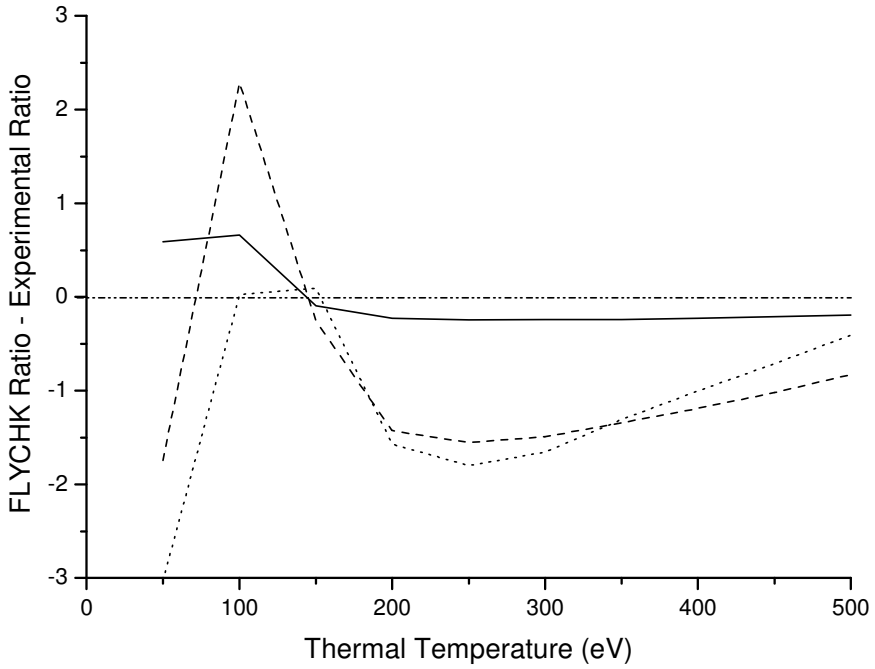

Figure 4. Plot of the difference between the satellite ratio determined via FLYCHK and our experimentally measured ratio for satellite lines qr/jkl (solid line), xy/jkl (dashed line), and xy/qr

(dotted line) as a function of thermal temperature. The case shown is for T_h=1keV and f=0.008 (best fit). The ratio differences indicate that T_c=140eV.

3.3 Spectral Line Profiles

It was found that He-like satellite spectra were best modelled using a double Gaussian line profile. The spectral profiles are strongly source broadened ($\lambda/\Delta\lambda \approx 400$), so the line profile represents a mapping of the spatial emission profiles of the lines, indicating two temperature regions. The superposition of source broadening effects due to a 25μm diameter plasma region of electron temperature T_h=1keV and a 120μm diameter region of electron temperature T_c=140eV is shown on figure 5 to fit the experimentally measured line profiles. The relative abundance of the number of hot and cold electrons used for this calculation is f=0.008, with intensity information obtained from FLYCHK. This relative abundance of hot and cold electrons is approximately consistent with the spatial dimensions of hot electrons (a circular region of radius r = 12μm) and cold electrons (a circular annulus region of radius between r =12μm and R = 60μm). Assuming uniform ablation, we would expect $f = \frac{\pi r^2}{\pi R^2 - \pi r^2} \cong 0.04$, but this could readily drop to f = 0.008 if the T_h value is produced late in the irradiation history or at limited spatial distance from the target surface. We discuss 2D simulations of the production of T_h and T_c in section 4.

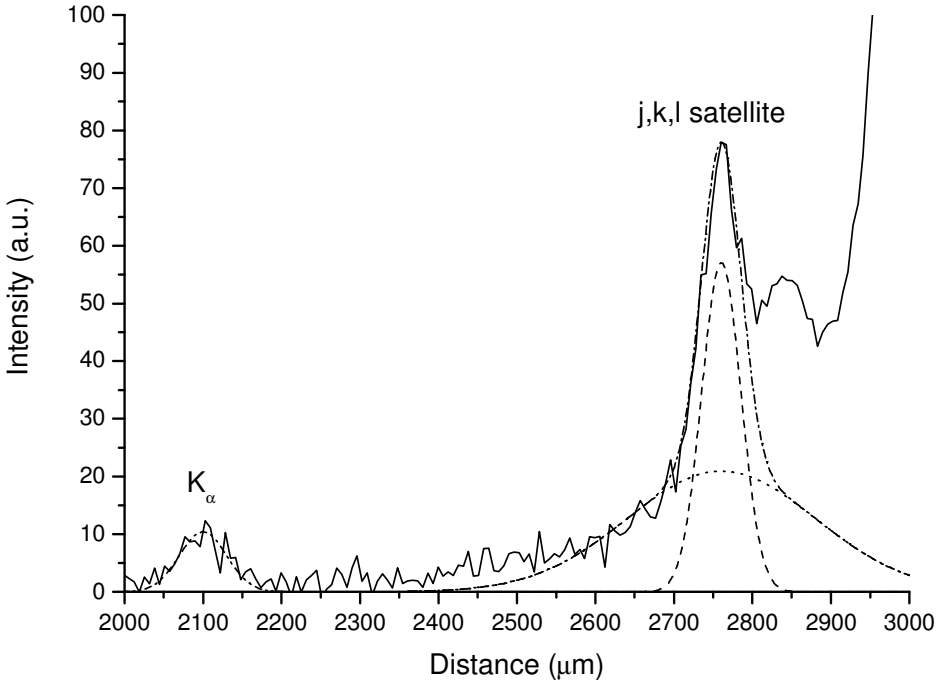

Figure 5. Expanded experimental spectrum as a function of distance on the CCD detector with a distance scale corresponding to the source broadening effect on the spectra. A double Gaussian profile for T_c=140eV and 120μm width at the target (dotted line) and of T_h=1keV and 25μm width at the target (dashed line) combine to form the emission profile observed. The K_α peak is best represented by a single Gaussian (dash-dot-dot line) with a spatial width of 60μm.

3.4 Al K_α Transmission Measurements

The spectrally integrated Al K_α intensity recorded by the spectrometer after transmission through the iron layer was measured for different laser pulse energies and directly compared with the integrated K_α signal originating from a pure Al target created using the same laser energy. A comparison of the transmitted and uninhibited spectra for a laser energy of 7.7J is shown in figure 6. Figure 7 demonstrates the change in transmission over the laser energy range investigated and shows a comparison to cold Fe transmission. It is seen that an increase in laser energy of 1.3 J causes sufficient additional heating to the iron layer through enhanced thermal conduction to produce an increase in transmission by almost a factor of 3.

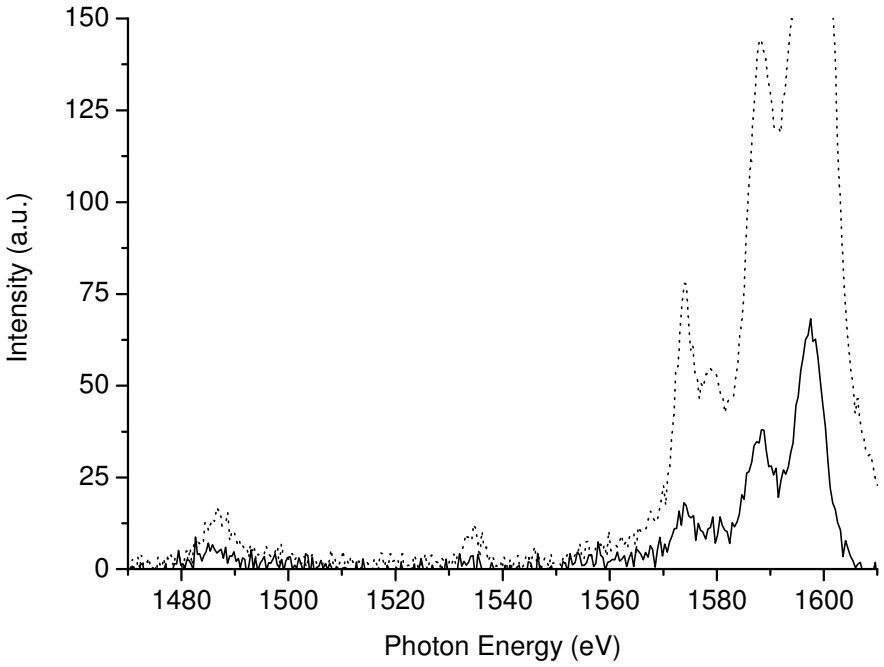

Figure 6. Experimentally observed, transmitted Al spectrum through an Fe plasma (solid line) and the spectrum from an aluminium target without iron (dotted line) for a laser energy of 7.7J.

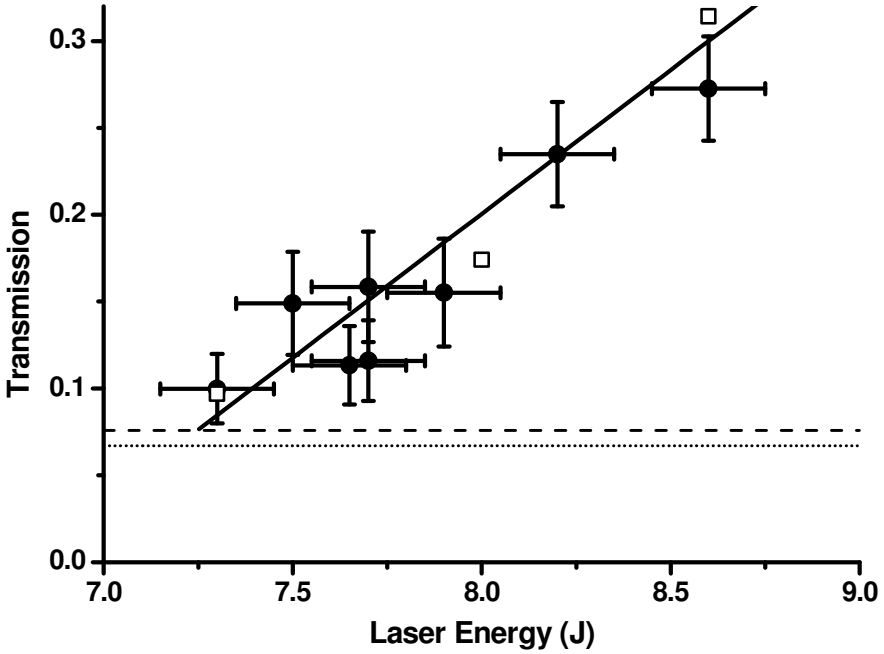

Figure 7. Transmission of K_α photons (1.5 keV) as a function of laser pulse energy as determined by experiment. Experimentally measured cold Fe transmission (dashed line) is compared with cold Fe transmission predicted (dotted line) by Henke et al. [9]. The open squares show calculated transmissions from h2d simulation, with line of best fit (solid line).

4. Simulation Results

The radiation hydrodynamic code h2d [16], was used to model the ablation and heating of the Al-Fe foil target. h2d models in 2D, the ablation, ionisation and expansion of material irradiated by a laser pulse to give the plasma density, temperature and ionisation as a function of distance and time in a Lagrangian coordinate system in *r,z* cylindrical geometry. The code incorporates multigroup diffusion of thermal radiation and flux limited electron conduction (flux limiter = 0.1 [17]). Laser absorption is by inverse bremsstrahlung with an energy dump of 20% at the critical density. To calculate the hydrodynamic variables in the evolving plasma, the SESAME equation of state package was used. The SESAME tables, developed by the T-1 group at Los Alamos National Laboratory, form a computer-based library of tables giving the thermodynamic properties of materials [18]. By post-processing the simulation output using opacity data from the IMP (Ionised Materials Package) code [19]; the transmission at the Al K_α wavelength through the Fe layer was calculated.

Our 2D h2d simulations assumed a cylindrical Al-Fe target of diameter 200 μm. The effect of a laser pulse incident on the Al surface with a 120 μm focal spot width and 500 ps duration with Gaussian time and spatial profiles was simulated for the experimental conditions. Figure 8 shows evidence for a central hot plasma of ≈ 1 - 1.6 keV with a surrounding cooler plasma of temperature ≈ 100 - 200 eV. These temperatures agree approximately with the 'two temperature' measurements found with our spectral fitting and diode measurements. An increase in laser energy causes an increase in the thermal self focusing effect (figure 8), causing an increase in the plasma temperature at the critical surface. This higher temperature region transfers more energy into the iron layer via thermal conduction, resulting in a higher Fe temperature, as shown in figure 10. The higher temperature results in a higher ionisation level in the Fe layer (above Fe XIX), so that direct photoionisation from the ground state of iron ions is not possible and the iron becomes transparent (see figure 7).

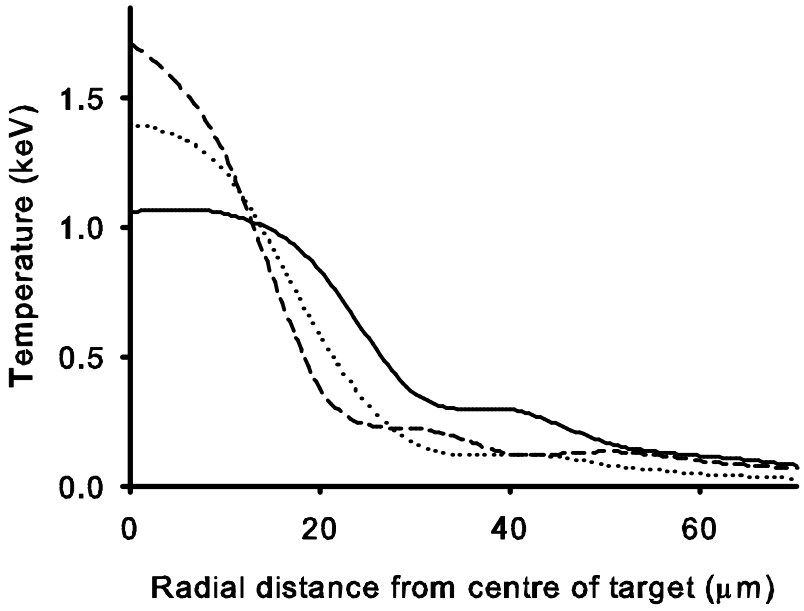

Figure 8. Radial temperature profiles for an ablated Al-Fe target from 2D h2d simulation with a 500 ps pulse incident on the Al surface. Shown are the simulated temperatures at the critical surface in the Al layer for a 7.3 J (solid line), 8 J (dotted line) and 8.6 J (dashed line) pulse at the time of the peak of the heating laser irradiance.

Al K_α emission was estimated from the 2D simulations (see figure 9). We assume that the total Al K_α emission, $\varepsilon_{K\alpha}$, comes from the electron collisional excitation rate coefficient, K, with Al atoms, at $E_{K\alpha}$ the Al K_α photon energy. We can write that

$$\varepsilon_{K\alpha} = n_i n_e K \propto n_e \int_{\sqrt{\frac{2E_{K\alpha}}{m}}}^{\infty} \sigma(v) v g_v(v) dv \tag{4}$$

where n_e is the electron density for the plasma, n_i is the solid Al atom density and g_v is the electron distribution function. The electron distribution function can be represented by a Maxwellian distribution $g_v(v)dv \propto \frac{v^2}{kT^{3/2}} exp(^{-mv^2}/_{2kT})dv$. The cross section, $\sigma(v)$, for K_α production is assumed constant for $E > E_{K\alpha}$[20]. Considering the relation in terms of energy and integrating gives

$$\varepsilon_{K\alpha} \propto n_e \left[\frac{E_{K\alpha}}{\sqrt{kT_e}} + \sqrt{kT_e}\right] exp(^{-E_{K\alpha}}/_{kT_e}) \tag{5}$$

where kT_e is the electron temperature. The emission of $\varepsilon_{K\alpha}$ is integrated axially and multiplied by the calculated transmission through the cells of the heated Fe layer to simulate the Al K_α flux through the target at the central radial position. The opacity in the Fe layer is calculated using the code predicted temperature and density and a look-up table of IMP tabulated opacities [19]. It can be seen that the peak of the transmitted Al K_α radiation is close to the peak laser irradiance on target (time '0', see figure 9). The K_α transmission at peak flux through the iron layer has been calculated for h2D simulations at different laser energies and was found to agree with the experimental transmission measurements (see figure 7).

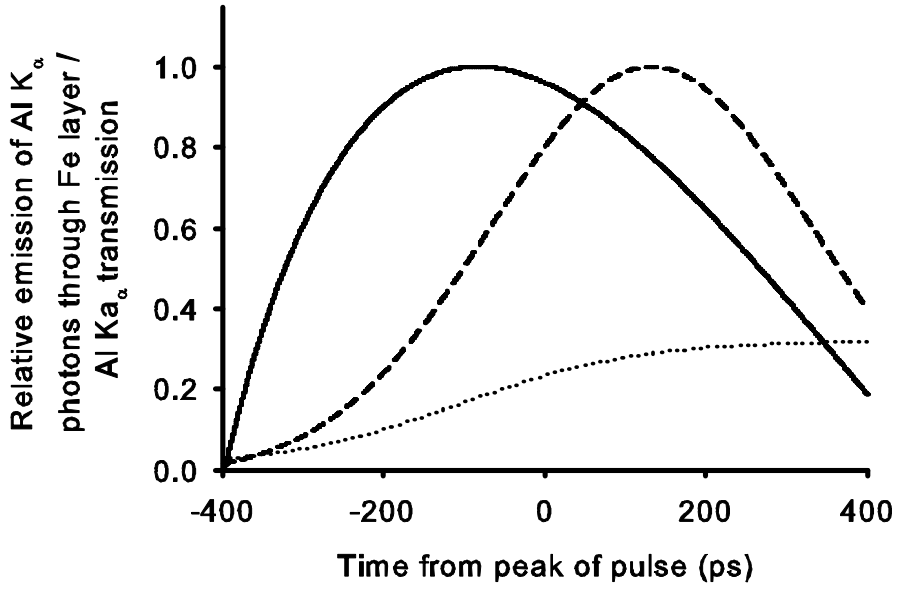

Figure 9. Flux of Al K_α photons through an Fe layer at the radial centre of the laser pulse, from 2D h2d simulation of the Al-Fe targets for a 7.3 J 500 ps laser pulse assuming a focal spot width of 120 μm (dashed line). The flux is the product of the emission of Al K_α from the Al layer (solid line) and transmission of Al K_α through the Fe layer (dotted line).

Further simulation has revealed predicted Fe temperatures at the time of peak Al K_α flux (see figure 9) range from 10 eV (back side of the target) to ≈ 70 eV (side closest to the laser) for a 7.3 J pulse and 20 eV to 150 eV for an 8.6 J pulse (see figure 10). The corresponding densities range between 0.2 gcm^{-3} and 1.1 gcm^{-3} for a 7.3 J pulse and between 0.1 gcm^{-3} and 0.8 gcm^{-3} for an 8.6 J pulse.

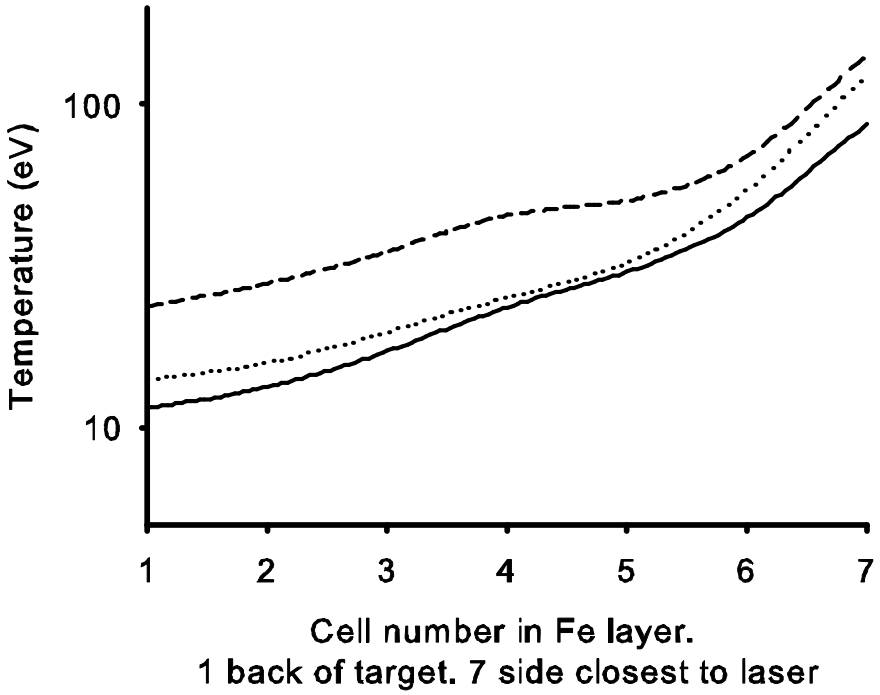

Figure 10. Axial temperature profiles, at the time of peak Al K_α flux, for the iron layer in an ablated Al-Fe target from h2d simulation with a 500 ps pulse incident on the Al surface with a pulse energy of 7.3 J (solid line), 8 J (dotted line) and 8.6 J (dashed line).

5. Discussion

Experimental temperature and K_α transmission data agree well with simulations using h2d and opacities from the Ionised Material Package (IMP). A two temperature spatially separate thermal distribution of electron temperatures, as observed here, has recently been reported by Colgan, et al [21].

Aluminium K_α emission has been used in this experiment as there has been a significant amount of previous study into the K_α spectra of aluminium, and the photon energy (1.49keV) results in photo-ionisation from the ground to continuum of Fe up to Fe XIX [22] so that there will be significant absorption of the radiation in iron plasmas up to electron temperatures ≈ 90eV. Once temperatures exceed ≈ 90eV, iron becomes close to transparent, so our K_α transmission measurements are a good diagnostic of temperatures > 90eV.

The assumption that Al K_α is emitted over a different timescale to that of other spectral lines, due to the hot electron interaction, has been checked by examining the transmission of He-like satellite lines through the iron. These lines were found to be more strongly transmitted by a factor of 2, compared with K_α transmission, suggesting more emission at later times when the iron transmission is greater.

The experiment has demonstrated the feasibility of performing opacity experiments using a table top laser system with modest parameters. Using this technique, we have been able to accurately characterise the Al back lighter and perform transmission measurements using a laser system with a high reproducibility (±10%) on a shot to shot basis. A number of issues need to be addressed to obtain high accuracy opacity information [23]. Simulations have demonstrated using this technique results in large temperature and density gradients in the axial and radial direction which would have to be accurately measured. Gradients in the axial direction can be reduced by introducing a plastic tamp layer on the rear side of the target, inhibiting the Fe plasma expansion, reducing the temperature gradient and providing conditions that can be validated more readily as LTE. Radial temperature gradients can be addressed by using a different heating mechanism than thermal self focussing. Using a shorter pulse length laser would prevent whole beam self focussing and could be optimised for resonance absorption to produce a higher number of hot electrons and to produce a shorter pulse back lighter. These hot electrons would increase the K_α signal and propagate into the Fe layer, heating the target, producing plasma with higher radial uniformity. The shorter pulse back lighter would provide better temporal resolution. Diagnosing the plasma conditions within the Fe layer has relied on using computer codes to simulate the thermal conduction from the front side Al plasma. An independent plasma diagnostic for the Fe layer is therefore required in order to determine the plasma conditions independently of hydrodynamic simulations. This could be achieved using absolute time gated imaging, probably in the visible, of the iron target to deduce a temperature assuming emission as a black-body.

6. Conclusion

A method for the characterisation of a plasma back lighter and the determination of plasma opacity using a single laser beam and a layered target has been investigated. Thermal conduction from laser produced aluminium plasma has been used as a heating mechanism for an iron target layer. K_α x-rays produced from the Al layer are used to measure transmission through the iron plasma. Whole-beam self focusing of the laser has reduced the effective spot size and increased the energy deposition into the iron. The temperature increase in the iron allows for opacity measurement over a temperature range ~ 10 – 150 eV. Combining source broadened spectroscopy with continuum emission analysis has enabled a plasma back lighter produced by whole beam self focussing to be characterised. The experimental data is in good agreement with 2D modelling using opacities from the Ionised Material Package code for 1.5 keV photon energy. Future work involves the use of hot electron heating of the Fe layer and the inclusion of a separate plasma diagnostic to determine the Fe plasma conditions.

Acknowledgements

The authors would like to thank Chris Spindloe (Rutherford Appleton Laboratory) for the target fabrication and the EPSRC for funding this work. We acknowledge the HiPER Project for funding of the HYADES and h2d codes, and Raoul Trines for the installations and maintenance of these codes.

References

[1] Rybicki G B and Lightman A P 1979 *Radiative Processes in Astrophysics,* (New York: Wiley) p 39

[2] Mínguez E, Martel P, Gil J M, Rubiano J G, and Rodríguez R 2002 *Fus. Eng. Des.* **60** 17-25

[3] Bailey J E, *et al* 2006 *Phys. Plasmas* **13** 056301

[4] Davidson S J, Foster J M, Smith C C, Warburton K A, and Rose S J 1988 *Appl. Phys. Lett.* **52** 847

[5] Perry T S, *et al* 1991 *Phys. Rev. Lett.* **67** 3784

[6] Edwards M H, *et al* 2006 *Phys. Rev. Lett.* **97** 035001

[7] Nazir K, Rose S J, Djaoui A, Tallents G J, Holden M G 1996 *Appl. Phys. Lett.* **69** 3686

[8] Nagler B, *et al* 2009 *Nature Physics* **5** 693-696

[9] Henke B L, Gullikson E M, and Davis J C 1993 *Atomic Data and Nuclear Data Tables* **54** 181-342

[10] Coe S E, Afshar-rad T, and Willi O 1990 *Europhys. Lett.* **13** 251-256

[11] Hutchinson I H 2002 *Principles of Plasma Diagnostics*, 2nd Edition (New York: Cambridge University Press)

[12] Gabriel A H 1972 *MNRAS* **160** 99

[13] Chung H -K, Chen M H, Morgan W L, Ralchenko Y, and Lee R W. 2005 *High Energy Density Physics* ***1*** *3-1***2**

[14] Ralchenko Yu, Kramida A E, Reader J, and NIST ASD Team 2008 *NIST Atomic Spectra Database* (version 3.1.5), [Online]. Available: http://physics.nist.gov/asd3 [2009, April 28]. National Institute of Standards and Technology, Gaithersburg, MD.

[15] Chung H K (private communication), Post-processor used to broaden theoretical FLYCHK spectra, NIST [received via email 21st Oct, 2008]

[16] Codes HYADES and h2d supplied by Cascade Applied Sciences, Inc. Jon Larsen, creator. Larsen@casinc.com.

[17] Bell A R, *et al* 2006 *Plasma Phys. Control. Fusion* **48** R37

[18] Lyon S P, Johnson J D 1992 Los Alamos National Laboratory Report LA-UR-92-3407

[19] Rose S J 1992 *J. Phys. B: At. Mol. Opt. Phys*. **25** 1667

[20] Reich C, *et al* 2000 *Phys. Rev. Lett.* **84** 4846

[21] Colgan J, Abdallah Jr., Fontes C J, Kilcrease D P, Dunn J, and Lee R W 2010 *Preprint* doi:10.1016/j.hedp.2010.01.015

[22] Corliss, C and Sugar, J 1982 *J. Phys. Chem. Ref. Data* **11** 135

[23] Perry T S, *et al* 1996 *Phys. Rev. E* **54** 5617